TECHNICAL NOTE

Evaluation of Corrosion Behavior of Ni/Be-Free Titanium-Based Metallic Glasses Fabricated by the Vacuum Arc Melting Method

Hossein Naseri, Behnam Lotfi*, Zohreh Sadeghian

* *behnaml@scu.ac.ir*

Department of Materials Science and Engineering, Faculty of Engineering, Shahid Chamran University of Ahvaz, Ahvaz, Iran

Received: July 2025 **Revised: October 2025** **Accepted: December 2025**
DOI: 10.22068/ijmse.4174

Abstract: *Bulk titanium-based metallic glass with an amorphous structure has led to the development of special properties that make it a suitable alternative to metallic biomaterials with a crystalline structure. In the present study, bulk titanium-based metallic glass without Ni and Be elements was produced by vacuum arc melting and cast into a 4 mm diameter mould. The evaluation of the results showed that the $Ti_{50}Zr_{15}Cu_{20}Mo_7Ag_4Sn_3Si_1$ metallic glass has a composite structure with dispersed crystalline phases (α-Ti, β-Ti, and Ti2Cu) within a glassy field. However, the $Ti_{50}Zr_{25}Cu_5Mo_{10}Ag_6Sn_3Si_1$ alloy has a higher glass formation ability (GFA), and the crystalline phases formed in the $Ti_{50}Zr_{15}Cu_{20}Mo_7Ag_4Sn_3Si_1$ alloy disappeared as the amounts of alloying elements Zr, Mo, and Ag increased. The corrosion current (I_{Corr}) of the $Ti_{50}Zr_{25}Cu_5Mo_{10}Ag_6Sn_3Si_1$ alloy (43.28 nA) was lower compared to the corrosion current of the $Ti_{50}Zr_{15}Cu_{20}Mo_7Ag_4Sn_3Si_1$ and Ti6Al4V samples (133.9 and 92.41 nA, respectively) in Hank's solution, hence the $Ti_{50}Zr_{25}Cu_5Mo_{10}Ag_6Sn_3Si_1$ alloy showed better corrosion resistance.*

Keywords: *Ti-Bulk metallic glasses, Glass formation ability, Corrosion behavior.*

1. INTRODUCTION

In recent years, Ti-based metallic glasses with high glass-forming ability (GFA) and interesting mechanical and chemical properties have been produced by vacuum casting. High glass-forming metallic glasses mean that the alloy in the molten state passes through the crystallization zone and transforms into a glassy (amorphous) state at the lowest cooling rate (sections of a few millimeters). However, many of the elements known to be involved in the production of metallic glasses are not necessarily biologically compatible. For example, many Ti-based metallic glasses with excellent GFA (large critical diameter) usually contain toxic elements such as Be, noble metals such as Pd and Pt, and intermediate elements such as Cu and Ni. Therefore, the presence of these elements has impaired the application prospects of Ti-based metallic glasses and has imposed limitations on the design of these metallic glasses [1, 2].

In general, in metallic glasses, the significant difference in negative heat of mixing (ΔHmix) and atomic radius (r) (at least 12%) between the base metal (here Ti) and other alloying elements is are essential parameters that increase the GFA [3, 4]. Elements that have negative heats of mixing with Ti include: Si, Mo, Pd, Sn, Pt, Be, Al, V, Fe, Co, Ni, Cu, Zn and Ag, among which only Si, Mo, Pd, Sn and Pt are biocompatible [5]. Also, elements that have significant atomic size mismatches (>12%) with Ti include: Si, Be, Fe, Co, Ni, and Cu, among which only Si are biocompatible [5]. Furthermore, the only elements that simultaneously satisfy both the metal glass formation parameters, namely negative heat of mixing (ΔHmix) and atomic radius (r) (at least 12%), are Si, Be, Fe, Co, Ni and Cu. Therefore, they can be considered as good glass formers for Ti-based alloys. Also, in a study by Chattopadhyay et al [6], it has been stated that, in addition to the negative enthalpy of mixing, the large number of alloy components and the atomic mismatch between the components, the viscosity factor can also be considered as an important kinetic property of the molten alloy for the formation of metallic glass, as it has a direct effect on the atomic rearrangement during rapid solidification. Hence, the alloying elements can be divided into two groups: high viscosity elements (Zr, Ti, Pd, Mo, Be and Si) and low viscosity elements (Al, Co, Fe, Ni, and Cu.) [6, 7].

Considering that most of the titanium-based BMGs previously reported in the literature [8, 9] contain Ni, Cu or Be, which are harmful to the human body, it seems that these elements are essential to achieve bulk metallic glass in titanium-based systems. Also, titanium-based metallic glasses

[DOI: 10.22068/ijmse.4174]

have recently been developed in several alloy systems, in which the elements Ni, Cu, and Be have been reduced [10-13]. Wang et al. [10] produced titanium-based metallic glass with the chemical composition $Ti_{47}Cu_{38-x}Zr_{7.5}Fe_{2.5}Sn_2Si_1Ag_2Pd_x$ (with Pd contents of 1 to 4 at.%) without highly toxic elements with a critical diameter of 4 to 5 mm. These researchers found that using Pd as a substitute for copper in the alloy improved ductility, reduced corrosion current density, and increased pitting potential. Zhou et al. [11] evaluated the thermal stability and crystallization behavior of the bulk metal glass $Zr_{70-x}Cu_{12.5}Ni_{10}Al_{7.5}Ag_x$ (x= 0-16). They found that the glass transition temperature (T_g) and the crystallization temperature (T_x) of the alloy shifted to higher temperatures with increasing Ag concentration. Also, the addition of Ag strongly affected the supercooled liquid zone (ΔT_x) and caused this zone to expand from 72 K to 110 K in the alloy containing 16 at. % Ag. Wang et al. [12] Successfully produced bulk metallic glasses with the chemical composition $Ti_{46}Cu_{31.5-x}Zr_{11.5}Co_7Sn_3Si_1Ag_x$ (x= 0, 1, 2, 3, 4, 5 at.%) in the form of rods up to 5 mm in diameter by vacuum casting. In this study, increasing the amount of the alloying element Ag from 0 to 5% caused the crystalline phases α-Ti, β-Ti, and Ti2Cu to disappear, resulting in a completely glassy alloy. Also, the increase in GFA in this alloy was attributed to a decrease in the melting temperature and an increase in the crystallisation activation energy caused by the addition of Ag. Quinn et al. [13] studied the effect of different alloying elements on the corrosion behavior of Ti-Cu-Ni-Zr alloy in NaCl and phosphate buffer solutions. They observed that the corrosion resistance was significantly improved by adding Nb or Ta. Effectively, Nb or Ta elements controlled the chemical composition of the passive film and facilitated its enrichment with titanium, thereby improving pitting corrosion resistance.

Despite these advancements, titanium-based BMGs still face critical challenges, including the high Cu content, susceptibility to pitting corrosion due to the formation of Ti-Cu intermetallic compounds, low titanium concentration (below 50 at.%), the use of expensive elements such as Pd, Pt, and Ta, and geometric limitations associated with thin-strip production via the melt spinning process [2]. Therefore, the development of titanium-based BMGs with enhanced corrosion resistance and improved biocompatibility requires replacing conventional alloying elements with those that maintain high glass-forming ability.

In the present paper, the aim is to produce titanium-based metallic glass free of toxic elements Ni and Be, and without expensive elements such as Pd, Pt and Ta, along with reducing the copper element and using molybdenum element (due to its high negative heat of mixing and viscosity) as a substitute for the copper element. In this research, $Ti_{50}Zr_{15}Cu_{20}Mo_7Ag_4Sn_3Si_1$ and $Ti_{50}Zr_{25}Cu_5Mo_{10}Ag_6Sn_3Si_1$ alloys (atomic percent) were produced by the vacuum arc melting method. The structure, microstructure and corrosion behavior of the samples were evaluated.

2. EXPERIMENTAL PROCEDURES

To fabricate the $Ti_{50}Zr_{15}Cu_{20}Mo_7Ag_4Sn_3Si_1$ and $Ti_{50}Zr_{25}Cu_5Mo_{10}Ag_6Sn_3Si_1$ alloys (at.%), high-purity elements (99.9%) were used. The alloying process was carried out via vacuum arc melting under an argon gas atmosphere. To ensure homogeneity, the melting process was repeated four times. In the final stage, the solidified ingot was remelted and cast into a water-cooled copper mould using vacuum suction casting, producing rods with a diameter of 4 mm and a length of 40 mm. To identify the phases present and analyze the microstructure resulting from the vacuum arc melting process, X-ray diffraction (XRD-Philip XXPERT-MPD) was performed over a scanning range of 20° to 90°. Additionally, field emission scanning electron microscopy (FE-SEM-LEO1455 VP) was employed to evaluate the microstructural characteristics of the fabricated samples. Electrochemical corrosion resistance of the Ti-based BMGs and the Ti6Al4V counterpart were characterized by electrochemical experiments with an electrochemical workstation (AutoLab potentiostat model Aut84091) in the Hank's solution (prepared by dissolving 8.00 g/L NaCl, 0.12 g/L $Na_2HPO_4.12H_2O$, 0.14 g/L $CaCl_2$, 0.35 g/L $NaHCO_3$, 0.20 g/L $MgSO_4.7H_2O$, 0.06 g/L KH_2PO_4, 1.00 g/L $C_6H_{12}O_6$, and 0.40 g/L KCl in the deionized water) at about 310 K. The working electrode, reference electrode, and counter electrode were the sample, Ag/AgCl, and platinum, respectively.

Potentiodynamic polarization curves were recorded at a scan rate of 0.1 V/s, ranging from -500 mV to +800 mV, after immersing the samples for 20 minutes, once the open-circuit potentials had stabilized.

[DOI: 10.22068/ijmse.4174]

3. RESULTS AND DISCUSSION

Fig. 1 presents the XRD patterns of 4 mm-diameter samples obtained by vacuum arc melting. As can be observed, the diffraction pattern of the $Ti_{50}Zr_{15}Cu_{20}Mo_7Ag_4Sn_3Si_1$ sample exhibits low-intensity peaks, indicating the presence of crystalline phases, mainly Ti and Ti_2Cu, while in the $Ti_{50}Zr_{25}Cu_5Mo_{10}Ag_6Sn_3Si_1$ alloy; the diffraction peaks related to the crystalline phases cannot be detected. The appearance of a broad halo typical of an amorphous structure in $Ti_{50}Zr_{25}Cu_5Mo_{10}Ag_6Sn_3Si_1$ shows better glass-forming ability of this alloy compared to that containing higher Cu content. It is worth mentioning that Ti_2Cu possesses a negative formation enthalpy of -8.6 $kJmol^{-1}$ (298 K) that is not highly negative. The enthalpy of mixing for alloys was calculated according to [11]:

$$\Delta H_{formation}^{glass} = \sum_i^j x_i . x_j \Delta H_{ij} \quad (1)$$

Where, $\Delta H_{ij} = x_i.x_j\ \emptyset(\Delta\emptyset.\Delta n.P)$, $\Delta\emptyset$ is the difference in electronegativity, Δn is the difference in electron density, P is the packing factor, and X is the molar fraction of elements. The enthalpies of mixing for $Ti_{50}Zr_{15}Cu_{20}Mo_7Ag_4Sn_3Si_1$ and $Ti_{50}Zr_{25}Cu_5Mo_{10}Ag_6Sn_3Si_1$ were determined to be -6.8 $kJmol^{-1}$ and -11.5 $kJmol^{-1}$, respectively. Considering the formation enthalpy of Ti_2Cu relative to the enthalpy of mixing, the formation of Ti2Cu in the $Ti_{50}Zr_{15}Cu_{20}Mo_7Ag_4Sn_3Si_1$ alloy can be expected. Formation of Ti_2Cu in metallic glass alloys containing high Cu and Ti content has been reported in previous studies, too [11]. Additionally, the atomic size mismatch between Mo and Ti is 6.7%, and that between Mo and Zr is 15%. These factors can be related to the suppression of intermetallic formation and the enhancement of the alloy GFA. This behavior has been observed in previous studies as well [14, 15]. Of course, it should be noted that in addition to the parameters affecting the formation of metal glass, which include negative enthalpy of mixing, large number of alloy components, and atomic mismatch between components, the viscosity factor can also be considered as an important kinetic property of the molten alloy for the formation of metal glass, because it has a direct effect on the atomic rearrangement in the cast alloy during rapid solidification [6]. Therefore, the use of alloying elements with high viscosity can affect the final viscosity of the produced alloy and increase the glass transition temperature. As can be seen in Fig. 1, the $Ti_{50}Zr_{25}Cu_5Mo_{10}Ag_6Sn_3Si_1$ alloy, due to its 10% at Mo alloying element, has shown better glass transition ability compared to the $Ti_{50}Zr_{15}Cu_{20}Mo_7Ag_4Sn_3Si_1$ alloy. The reason for this is the high viscosity of Mo relative to Cu, which increases the viscosity of the final alloy and thus acts as a barrier to atomic rearrangement during solidification. In other words, the high content of the alloying element Mo in the $Ti_{50}Zr_{25}Cu_5Mo_{10}Ag_6Sn_3Si_1$ alloy facilitates the stability of the supercooled liquid and prevents the formation of crystal nuclei during solidification [6, 7]. According to the aforementioned phenomena, the formation of Ti2Cu in $Ti_{50}Zr_{15}Cu_{20}Mo_7Ag_4Sn_3Si_1$ can be attributed to both a more negative heat of intermetallic formation and a lower alloy viscosity, which facilitates the nucleation of crystalline phases. The formation of crystals can be considered to provide nucleation sites for the crystallisation of other phases, such as Ti solid solutions.

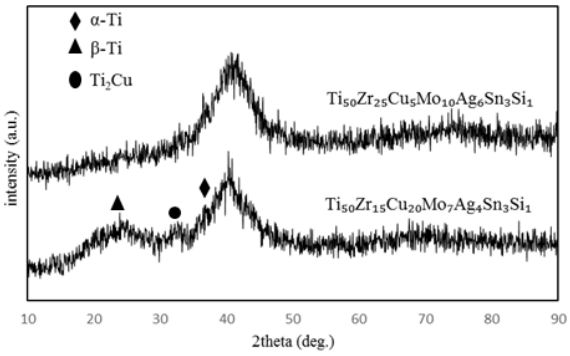

Fig. 1. XRD patterns obtained from rod-shaped samples with a diameter of 4 mm of a) $Ti_{50}Zr_{15}Cu_{20}Mo_7Ag_4Sn_3Si_1$ and b) $Ti_{50}Zr_{25}Cu_5Mo_{10}Ag_6Sn_3Si_1$

FE-SEM microstructural images and EDS analysis of bulk $Ti_{50}Zr_{15}Cu_{20}Mo_7Ag_4Sn_3Si_1$ and $Ti_{50}Zr_{25}Cu_5Mo_{10}Ag_6Sn_3Si_1$ alloys are presented in Fig. 2. As shown in Fig. 2a, the microstructure of $Ti_{50}Zr_{15}Cu_{20}Mo_7Ag_4Sn_3Si_1$ consists of a gray dendritic phase with a black phase distributed at the boundaries of the dendrites, and bright white particles scattered throughout the gray dendritic phase. According to the EDS analysis, it can be seen that points A and B have a higher titanium content, which indicates the α-Ti and β-Ti phases, respectively [16]. While the atomic percentage of titanium at point C is approximately twice that of copper, according to the XRD pattern performed on the $Ti_{50}Zr_{15}Cu_{20}Mo_7Ag_4Sn_3Si_1$ alloy, this crystalline phase has been identified as Ti_2Cu (Fig. 2c–f) [10]. However, with the addition of 10 at.% Mo (Fig. 2-b), the crystalline phases could not be detected

[DOI: 10.22068/ijmse.4174]

in the microstructure of the $Ti_{50}Zr_{25}Cu_5Mo_{10}Ag_6Sn_3Si_1$ sample. Regarding microstructural changes, reducing the amount of the alloying element Cu and adding other elements, such as Mo, can effectively reduce or eliminate the nucleation and growth of crystalline phases during solidification, due to the increase in alloy viscosity. In this way, the ability to form metallic glass in the $Ti_{50}Zr_{25}Cu_5Mo_{10}Ag_6Sn_3Si_1$ alloy has been greatly increased. Similar results have been reported in previous research, too [12, 17]. Shrinkage porosity is also observed in Fig 2. The pores are likely formed by the coalescence of free volume during rapid solidification, which tends to trap nanoscale voids as the material vitrifies. As the rapid cooling prevents dense atomic packing in metallic glasses, free volume arises, and under certain conditions, these regions can cluster and stabilize into pores [18, 19].

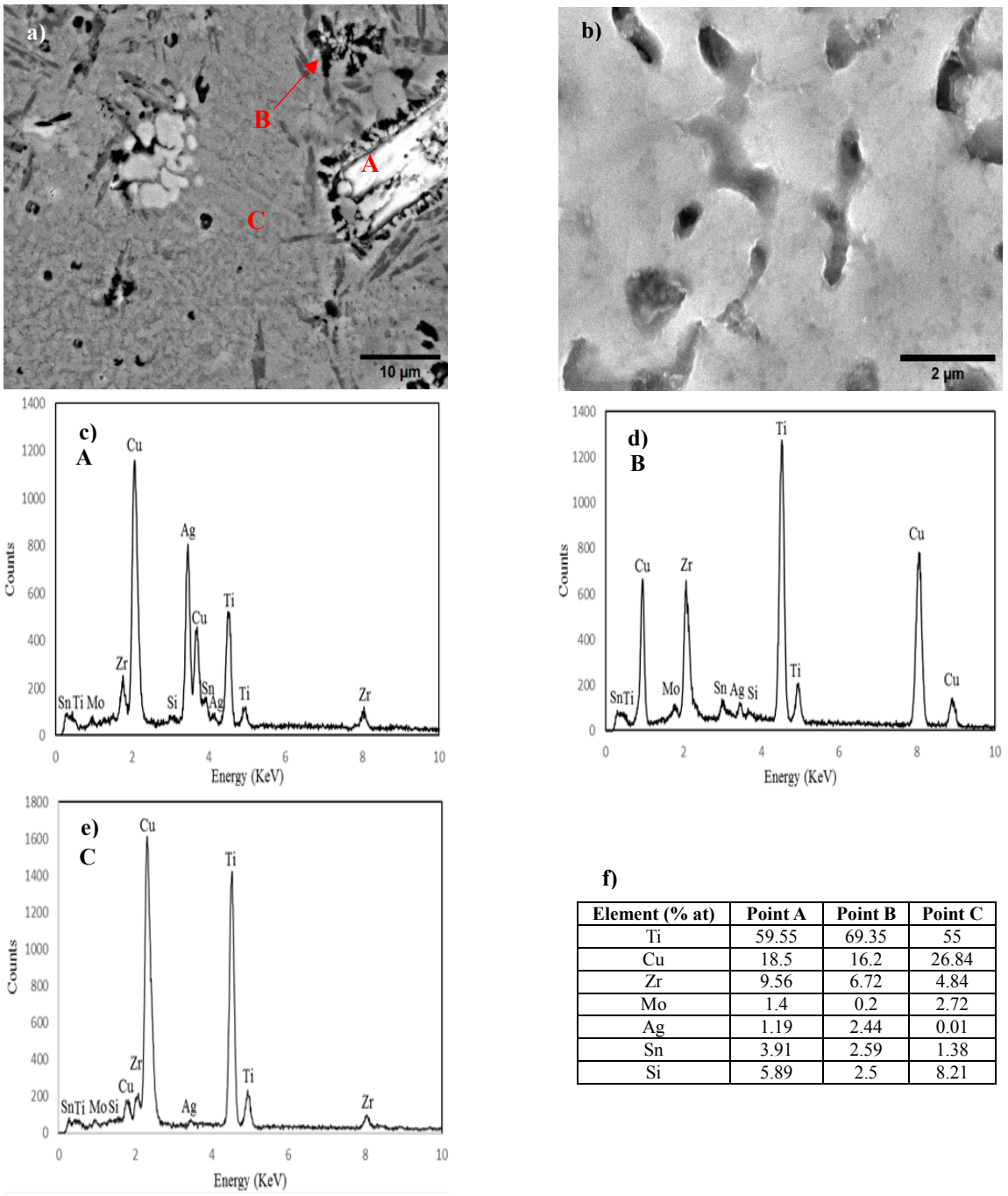

f)

Element (% at)	Point A	Point B	Point C
Ti	59.55	69.35	55
Cu	18.5	16.2	26.84
Zr	9.56	6.72	4.84
Mo	1.4	0.2	2.72
Ag	1.19	2.44	0.01
Sn	3.91	2.59	1.38
Si	5.89	2.5	8.21

Fig. 2. Electron microscope image of different alloys a) $Ti_{50}Zr_{15}Cu_{20}Mo_7Ag_4Sn_3Si_1$ and b) $Ti_{50}Zr_{25}Cu_5Mo_{10}Ag_6Sn_3Si_1$, c-f) EDS analysis of different areas in the $Ti_{50}Zr_{15}Cu_{20}Mo_7Ag_4Sn_3Si_1$ alloy

[DOI: 10.22068/ijmse.4174]

The bio-corrosion performance of $Ti_{50}Zr_{15}Cu_{20}Mo_7Ag_4Sn_3Si_1$ and $Ti_{50}Zr_{25}Cu_5Mo_{10}Ag_6Sn_3Si_1$ alloys, along with Ti6Al4V alloy, as a widely used alloy in biomaterial applications, was investigated by measuring the electrochemical corrosion activity in Hank's solution (simulated body fluid). The potentiodynamic polarization curves of the tested samples and the corrosion test results are shown in Fig. 3 and Table. 2, respectively. It can be seen from Figure 3 that the $Ti_{50}Zr_{25}Cu_5Mo_{10}Ag_6Sn_3Si_1$ alloy has spontaneous passive behavior, while no passive film was formed on the surface of the $Ti_{50}Zr_{15}Cu_{20}Mo_7Ag_4Sn_3Si_1$ and Ti6Al4V alloys under the test conditions. $Ti_{50}Zr_{25}Cu_5Mo_{10}Ag_6Sn_3Si_1$ alloy exhibits a lower corrosion current (I_{Corr}) than the $Ti_{50}Zr_{15}Cu_{20}Mo_7Ag_4Sn_3Si_1$ and Ti_6Al_4V alloys (Table 2). This can be attributed to the homogeneity of the metallic glass structure, which is one of the main characteristics of its high resistance to corrosive environments.

However, in the $Ti_{50}Zr_{15}Cu_{20}Mo_7Ag_4Sn_3Si_1$ alloy, the presence of crystalline phases dispersed within the metallic glass field was essential for reducing corrosion resistance. In other words, the presence of phase boundaries in the structure of this alloy itself is considered as a preferred location for the initiation of corrosion [12, 13, 20]. Also, the $Ti_{50}Zr_{25}Cu_5Mo_{10}Ag_6Sn_3Si_1$ alloy has a lower corrosion current density (I_{corr}) of 43.28 nA than the Ti_6Al_4V alloy. This can be attributed to the absence of crystal defects (grain boundaries) and to the formation of a uniform passive film on the surface of the $Ti_{50}Zr_{25}Cu_5Mo_{10}Ag_6Sn_3Si_1$ alloy.

Considering that the corrosion behavior of BMG alloys is closely related to their chemical composition, the higher corrosion resistance of $Ti_{50}Zr_{25}Cu_5Mo_{10}Ag_6Sn_3Si_1$ alloy compared to $Ti_{50}Zr_{15}Cu_{20}Mo_7Ag_4Sn_3Si_1$ alloy can be explained as follows. Depending on the chemical elements present in the passive film, the affinity for chloride ions may vary. In general, the presence of Cu alloying in the metallic glass reduces the resistance of the passive film formed on the surface of the test samples. In other words, in systems with high Cu alloying element content, Cu ions tend to separate from the passive film and accumulate at the substrate-film interface. Subsequently, Cu ions are released and chloride ions in the solution combine to form $CuCl^{2-}$ corrosion products, which cause instability and thinning of the protective layer and lead to more pitting corrosion in Ti-based metallic glasses [21]. Therefore, the presence of Cu in large amounts (20 at%) in the $Ti_{50}Zr_{15}Cu_{20}Mo_7Ag_4Sn_3Si_1$ alloy prevented the formation of a protective film on the sample surface and increased the pitting corrosion mechanism in this alloy. In contrast, the formation of a protective film in the $Ti_{50}Zr_{25}Cu_5Mo_{10}Ag_6Sn_3Si_1$ alloy can be attributed to the reduction in the amount of copper alloying element, because with less copper, the thinning of the protective layer, caused by the separation of copper ions, has decreased. Also, the presence of the alloying element Mo in the $Ti_{50}Zr_{25}Cu_5Mo_{10}Ag_6Sn_3Si_1$ alloy leads to the formation of a stable passive MoO_3 layer, which improves the corrosion resistance and pitting of metallic glass [22]. Therefore, one reason for the improved corrosion resistance of the $Ti_{50}Zr_{25}Cu_5Mo_{10}Ag_6Sn_3Si_1$ alloy compared to the $Ti_{50}Zr_{15}Cu_{20}Mo_7Ag_4Sn_3Si_1$ alloy is the increase in Mo content and the decrease in Cu content. Another reason that can be mentioned is the presence of Cl^- ions in Hank's solution, which readily penetrate the oxide layer's defects, accelerate the destruction of the protective layer, and increase the pitting corrosion mechanism. Considering that the $Ti_{50}Zr_{15}Cu_{20}Mo_7Ag_4Sn_3Si_1$ alloy has a mixed structure of crystalline phases dispersed in a glassy matrix, the formation of microgalvanic cells between them prevents the formation of a uniform oxide layer and causes the formation of a non-uniform protective film on the surface of this sample.

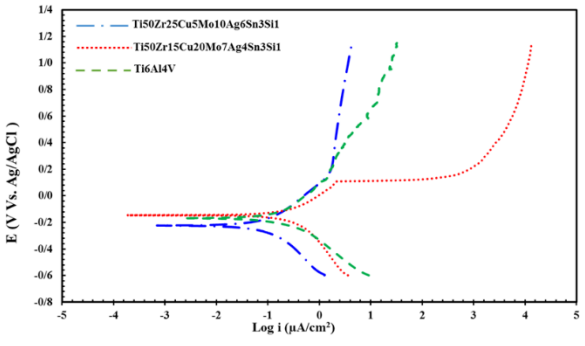

Fig. 3. Polarization curves of different samples in Hank's solution

Table 1. Polarization corrosion test results in Hank's solution

Sample	E_{Corr} (V vs. SCE)	I_{Corr} (nA)	Corrosion rate (mpy)
$Ti_{50}Zr_{15}Cu_{20}Mo_7Ag_4Sn_3Si_1$	-145.69	133.9	0.0024
$Ti_{50}Zr_{25}Cu_5Mo_{10}Ag_6Sn_3Si_1$	-223.52	43.28	0.0012
Ti6Al4V	-168.2	92.41	0.00134

[DOI: 10.22068/ijmse.4174]

Therefore, the low corrosion resistance of the $Ti_{50}Zr_{15}Cu_{20}Mo_7Ag_4Sn_3Si_1$ alloy can be attributed to the rapid destruction of the protective layer by Cl^- ions.

4. CONCLUSIONS

Bulk $Ti_{50}Zr_{15}Cu_{20}Mo_7Ag_4Sn_3Si_1$ and $Ti_{50}Zr_{25}Cu_5Mo_{10}Ag_6Sn_3Si_1$ alloys (at.%) were produced by vacuum arc melting process. $Ti_{50}Zr_{15}Cu_{20}Mo_7Ag_4Sn_3Si_1$ alloy exhibited a partially glassy structure with α-Ti, β-Ti, and Ti_2Cu crystalline phases dispersed in the glassy matrix. With decreasing Cu and increasing the amounts of Zr, Mo, and Ag alloying elements in the $Ti_{50}Zr_{25}Cu_5Mo_{10}Ag_6Sn_3Si_1$ alloy, no crystalline phases could be detected. It was concluded that glass formation ability improved by reducing Cu and increasing elements like Mo that with increasing alloy viscosity, confined the rearrangement of elements and decelerated nucleation. The $Ti_{50}Zr_{25}Cu_5Mo_{10}Ag_6Sn_3Si_1$ alloy with a corrosion current (I_{Corr}) of 43.28 nA has better corrosion resistance compared to the $Ti_{50}Zr_{15}Cu_{20}Mo_7Ag_4Sn_3Si_1$ alloy with a corrosion current of 133.9 nA. In addition, the $Ti_{50}Zr_{25}Cu_5Mo_{10}Ag_6Sn_3Si_1$ alloy has shown better corrosion behavior in the body simulation solution (Hank) than the Ti6Al4V alloy with a corrosion current of 41.92 nanoamperes, so it can be expected that this metallic glass can be a suitable replacement for the widely used Ti6Al4V alloy.

REFERENCES

[1] Zhang, M., et al., A Brief introduction on the development of Ti-based metallic glasses. Frontiers in Materials, 2022. 8: p. 814629.

[2] Lin, B., et al., Enhanced wear, corrosion, and corrosive-wear resistance of the biocompatible Ti-based bulk metallic glass by oxidation treatment. Journal of Non-Crystalline Solids, 2022. 576: p. 121231.

[3] Kuball, A., et al., Development and characterization of titanium-based bulk metallic glasses. Journal of Alloys and Compounds, 2019. 790: p. 337-346.

[4] Guo, Y., et al., Ni-and Cu-free Ti-based metallic glasses with potential biomedical application. Intermetallics, 2015. 63: p. 86-96.

[5] Calin, M., et al., Designing biocompatible Ti-based metallic glasses for implant applications. Materials Science and Engineering: C, 2013. 33(2): p. 875-883.

[6] Chattopadhyay, C. and B. Murty, Kinetic modification of the 'confusion principle' for metallic glass formation. Scripta Materialia, 2016. 116: p. 7-10.

[7] Ishikawa, T., et al., Viscosity of molten Mo, Ta, Os, Re, and W measured by electrostatic levitation. The Journal of Chemical Thermodynamics, 2013. 65: p. 1-6.

[8] Li, Q., et al., Mechanical and corrosion properties of Ti-Ni-Cu-Zr metallic glass matrix composites. Journal of Alloys and Compounds, 2017. 727: p. 1344-1350.

[9] Wu, X., et al., Bulk metallic glass formation in a ternary Ti–Cu–Ni alloy system. Journal of Alloys and Compounds, 2008. 452(2): p. 268-272.

[10] Wang, C., et al., Ti-Cu-Zr-Fe-Sn-Si-Ag-Pd bulk metallic glasses with potential for biomedical applications. Metallurgical and Materials Transactions A, 2021. 52: p. 1559-1567.

[11] Zhou, W., et al., Effect of Ag content on thermal stability and crystallization behavior of Zr–Cu–Ni–Al–Ag bulk metallic glass. Journal of Non-Crystalline Solids, 2015. 411: p. 132-136.

[12] Wang, T., et al., Novel Ti-based bulk metallic glasses with superior plastic yielding strength and corrosion resistance. Materials Science and Engineering: A, 2015. 642: p. 297-303.

[13] Qin, F., et al., Corrosion behavior of Ti-based metallic glasses. Materials transactions, 2006. 47(8): p. 1934-1937.

[14] Liens, A., et al., Effect of alloying elements on the microstructure and corrosion behavior of TiZr-based bulk metallic glasses. Corrosion Science, 2020. 177: p. 108854.

[15] Zhou, Q., et al., Identifying the significance of Sn addition on the tribological performance of Ti-based bulk metallic glass composites. Journal of Alloys and Compounds, 2019. 780: p. 671-679.

[16] Motyka, M., et al., Characterization of the Interface Between α and β Titanium Alloys in the Diffusion Couple. Metallurgical and Materials Transactions A, 2020. 51: p. 6584-6591.

[17] Liu, Y., et al., Tribological behaviors of a Ni-free Ti-based bulk metallic glass in air and a simulated physiological environment. Journal of Alloys and Compounds, 2018. 766: p. 1030-1036.

[DOI: 10.22068/ijmse.4174]

[18] Chang, Y., et al., Effect of cast process and microalloying on the fracture toughness of Zr-based bulk amorphous alloys. Journal of alloys and compounds, 2014. 614: p. 87-93.
[19] Srivastava, A.P., et al., Elimination of porosity in bulk metallic glass castings using hot isostatic pressing. Journal of Non-Crystalline Solids, 2017. 468: p. 5-11.
[20] Khadempir, S.E., B. Lotfi, and Z. Sadeghian, Effect of Current Type and Particle Size on Wear and Corrosion Behaviour of Electro-plated Ni-B4C Composite Coatings. Iranian Journal of Materials Science & Engineering, 2025. 22(3).
[21] Fernández-Navas, N., et al., Electrochemical surface nanostructuring of $Ti_{47}Cu_{38}Fe_{2.5}Zr_{7.5}Sn_2Si_1Ag_2$ metallic glass for improved pitting corrosion resistance. Advanced Engineering Materials, 2024. 26(11): p. 2302206.
[22] Cheng, X., et al., Effect of Mo addition on the properties of Fe-Co-Zr-WB bulk metallic glasses. Journal of Non-Crystalline Solids, 2022. 587: p. 121587.

[DOI: 10.22068/ijmse.4174]